01,10

Nonlinear acoustic effects in polycrystalline solids with saturation of amplitude-dependent internal friction

© V.E. Nazarov, S.B. Kiyashko

Institute of Applied Physics, Russian Academy of Sciences,
Nizhny Novgorod, Russia

E-mail: v.e.nazarov@appl.sci-nnov.ru

Received April 26, 2022
Revised May 26, 2022
Accepted May 17, 2022

Theoretical and numerical studies of nonlinear acoustic effects arising from the propagation of initially harmonic waves in polycrystalline solids with saturation of amplitude-dependent internal friction have been carried out. Two main types of hysteresis are considered: elastic and inelastic. A comparative analysis of the regularities of nonlinear effects is carried out and the characteristics of nonlinear quasi-harmonic waves in such media are determined: amplitude-dependent losses and changes in propagation velocity, as well as amplitudes of higher harmonics. A method for determining the type of polycrystal hysteresis based on the analysis of theoretical and experimentally established amplitude dependences of nonlinear effects is proposed.

Keywords: elastic waves, amplitude-dependent internal friction.

DOI: 10.21883/PSS.2022.08.54694.365

1. Introduction

The propagation of elastic waves in various media is accompanied by a variety of nonlinear acoustic effects (NAE): nonlinear attenuation and phase velocity changes, secondary wave generation at frequencies of combinational harmonics, waveform distortion, etc. In micro-inhomogeneous solids with strong nonlinearity, NAEs appear more intensively (than in homogeneous weakly nonlinear media), and their patterns are determined by the nonlinearity of the equation of state of the medium, i.e. dependence $\sigma = \sigma(\varepsilon)$, where σ and ε — stress and strain. In turn, the equations of state of micro-inhomogeneous solids are determined by nonlinear defects in their structure (dislocations, grains, cracks, etc.) and are characterized by various types of non-analytic nonlinearity: elastic, hysteresis, and inelastic. Many polycrystalline metals, alloys and rocks are classified as strongly nonlinear micro-inhomogeneous solids. In connection with the widespread occurrence of such materials, theoretical studies of NAEs in micro-inhomogeneous media with different types of nonlinearity are relevant and necessary when analyzing the results of relevant experiments carried out to establish the physical mechanisms of anomalously high nonlinearity of such media and to obtain their dynamic equations of state.

When intense elastic oscillations and waves are excited in polycrystalline solids, dislocation amplitude-dependent internal friction (ADIF) occurs, which leads to nonlinear damping decrement (DD) and elastic modulus defect (EMD) [1–11]. The ADIF phenomenon is explained within the framework of hysteresis equations of state. The results of experimental studies show that as the amplitude of the elastic oscillations in some metals (copper [5,12,13], aluminum [14,15], indium [16,17], zinc [18], lead [19]) increases, saturation of hysteresis DD and EMD occurs. (Generally speaking, hysteresis behavior is characteristic not only of the mechanical properties of polycrystals, but also of the magnetic and dielectric properties of ferromagnets and ferroelectrics, with saturation effects [20,21] also occurring for them. The nature and physical mechanisms of the different hysteresis are different, but their phenomenological description contains much in common).

Two basic types of hysteresis are used to describe the effects of ADIF in polycrystals: elastic (or breakaway hysteresis) and inelastic (frictional or plastic hysteresis) [22,23]. For elastic hysteresis — $\sigma(\varepsilon = 0) = 0$, and for inelastic — $\sigma(\varepsilon = 0) \neq 0$. Examples of elastic and inelastic hysteresis are the Granato–Lücke hysteresis [3] and the Davidenkov hysteresis [1] respectively. Generally speaking, the two hysteresis accounts for the effects of ADIF — the decrement in damping and the defect in modulus of elasticity, but these hysteresis have some differences. They appear in the study of patterns of ADIF effects and the generation of higher harmonics arising from the propagation in hysteresis media of intense initially harmonic waves (IHW). Thus, one of the main issues in the analytical description of ADIF is the adequate choice of the hysteresis equation of state for the solid under study. Although the use of hysteresis equations to describe the effects of ADIF in polycrystals is not in doubt, the adequacy of this choice presents a rather difficult and topical problem. However, based on the analysis of the amplitude dependences of the NAE experimentally determined for a particular hysteresis material, the type of hysteresis for this material can be determined. This requires knowledge of the patterns of NAE in solids with different types of hysteresis, including saturation effects ADIF.

In this paper, theoretical and numerical studies are carried out on the NAE arising from IHW propagation in hysteresis solids with ADIF saturation. Two types of quadratic hysteresis are considered here: elastic and inelastic. A comparative analysis of the patterns of nonlinear effects has been carried out and the characteristics of nonlinear quasi harmonic waves in such media have been determined: amplitude-dependent losses and changes in propagation velocity as well as amplitudes of second and third harmonics have been determined. Based on the analysis and correspondence of analytical and experimentally determined NAE amplitude dependences the method of hysteresis type determination for polycrystalline solids has been proposed.

2. Hysteresis equation of state for solid bodies with saturation ADIF

The nonlinear equation of state for a solid is given in the following form:

$$\sigma(\varepsilon) = E[\varepsilon - f(\varepsilon)], \tag{1}$$

where E — elastic modulus, $f(\varepsilon)$ — nonlinear (here hysteresis) function, $|f(\varepsilon)| \ll |\varepsilon| < |\varepsilon_{\text{th}}| \ll 1$, $|f_\varepsilon(\varepsilon)| \ll 1$, $|\sigma| < |\sigma_{\text{th}}|$, $\sigma_{\text{th}} = E\varepsilon_{\text{th}}$ — the maximum stress (limit of elasticity) beyond which irreversible plastic deformation occurs in a solid; for many materials $|\varepsilon_{\text{th}}| > 10^{-4}$–$10^{-3} \ll 1$.

Experimental studies of ADIF for longitudinal elastic waves containing compression ($\varepsilon < 0$) and tension ($\varepsilon > 0$) phases show that at not very large strain amplitudes, when there is no saturation of ADIF effects, for many polycrystalline metals (e.g., copper [12], zinc [18], lead [19]) and rocks (granite, magnesite, limestone) [24] — $f(\varepsilon) \propto \varepsilon^2$. Such studies also show that for these polycrystals the amplitude-dependent EMD and DD are determined by different nonlinearity parameters and, therefore, for longitudinal stresses σ and strains ε the hysteresis in the $\sigma = \sigma(\varepsilon)$ relation consists of square, but generally speaking, asymmetric branches.

For an elastic quadratic hysteresis similar to the Granato–Lücke [3] hysteresis, and accounting for EMD and DD saturation, the function $f(\varepsilon)$ is

$$f(\varepsilon) = \frac{1}{2(1+\gamma_0|\varepsilon|)} \times \begin{cases} \gamma_1\varepsilon^2, & \varepsilon \geq 0,\ \dot{\varepsilon} > 0, \\ -\gamma_2\varepsilon^2 + (\gamma_1+\gamma_2)\varepsilon_m\varepsilon, & \varepsilon \geq 0,\ \dot{\varepsilon} < 0, \\ -\gamma_3\varepsilon^2, & \varepsilon \leq 0,\ \dot{\varepsilon} < 0, \\ \gamma_4\varepsilon^2 + (\gamma_3+\gamma_4)\varepsilon_m\varepsilon, & \varepsilon \leq 0,\ \dot{\varepsilon} > 0, \end{cases} \tag{2}$$

where ε_m — strain amplitude, $\gamma_{0,1-4}$ — dimensionless nonlinearity parameters,$\gamma_0 \geq 0$, $\gamma_1 + \gamma_2 \geq 0$, $\gamma_3 + \gamma_4 \geq 0$, $|\gamma_{1-4}\varepsilon_m| \ll 1$. (Generally speaking, $\gamma_1 \neq \gamma_2 \neq \gamma_3 \neq \gamma_4$.) In Granato–Lucke's theory, polycrystalline hysteresis is associated with periodic detachment of dislocations from impurity atoms (and subsequent attachment to them) under the action of an external alternating stress.

For an inelastic quadratic hysteresis similar to the Davidenkov hysteresis [1], and accounting for EMD saturation and DD, the function $f(\varepsilon)$ is

$$f(\varepsilon) = \frac{\beta\varepsilon_m\varepsilon}{1+\alpha_1|\varepsilon|} + \frac{1}{2(1+\alpha_2|\varepsilon|)} \times \begin{cases} \beta_1\varepsilon^2 - \frac{\beta_1+\beta_2}{2}\varepsilon_m^2, & \dot{\varepsilon} > 0; \\ -\beta_2\varepsilon^2 + \frac{\beta_1+\beta_2}{2}\varepsilon_m^2, & \dot{\varepsilon} < 0, \end{cases} \tag{3}$$

where $\alpha_{1,2}, \beta, \beta_{1,2}$ — nonlinearity parameters,$\alpha_{1,2} \geq 0$, $\beta_1 + \beta_2 \geq 0$, $|\beta|\varepsilon_m \ll 1$, $|\beta_{1,2}|\varepsilon_m \ll 1$. (Generally speaking, $\alpha_1 \neq \alpha_2$, $\beta \neq \beta_1 \neq \beta_2$.) At $\alpha_{1,2} = 0$ and $\beta = \beta_1 = \beta_2$ equations (1), (3) describe a symmetric quadratic Davidenkov hysteresis (to be precise in notation, it coincides with the Rayleigh ferromagnetic hysteresis [21,25]). In equation (3), the first (non-hysteresis) term defines the EMD and the second (hysteresis) — DD. The Davidenkov model relates the hysteresis behavior of a solid to its microplastic deformation [1] caused by the reversible displacement of dislocation under the action of an external alternating stress. (In work [26] a similar hysteresis was considered, in which the saturation of ADIF effects is determined by the multiplier $(1+\alpha_0\varepsilon_m)^{-1} \leq 1$, $\alpha_0 \geq 0$).

In polycrystals with elastic hysteresis (2), the same multiplier $(1+\gamma_0|\varepsilon|)^{-1} \leq 1$ is responsible for EMD and DD saturation, while with inelastic (3) — two different ones: $(1+\alpha_1|\varepsilon|)^{-1} \leq 1$ and $(1+\alpha_2|\varepsilon|)^{-1} \leq 1$. Hysteresis (2), (3) and at $\gamma_0 = 0$, $\alpha_{1,2} = 0$ (no saturation) and at $\gamma_0\varepsilon_m > 1$, $\alpha_{1,2}\varepsilon_m > 1$ (saturation) are significantly different, so the patterns of NAE in solids with such hysteresis, will be different. The hysteresis (2), (3) consist of four branches ($\varepsilon \geq 0$, $\dot{\varepsilon} > 0$, $\varepsilon \geq 0$, $\dot{\varepsilon} < 0$, $\varepsilon \leq 0$, $\dot{\varepsilon} < 0$, $\varepsilon \leq 0$, $\dot{\varepsilon} > 0$) converging to each other at $\varepsilon = 0$ and $\varepsilon = \pm\varepsilon_m$. The qualitative view of these hysteresis at $\gamma_0 = 0$, $\alpha_{1,2} = 0$ and $\gamma_0 > 0$, $\alpha_{1,2} > 0$ is shown in Fig. 1, which shows that as the parameters γ_0 and $\alpha_{1,2}$ increase, the hysteresis loop shapes change, with their area and slope decreasing, corresponding to saturation effects of ADIF.

In [14,27], in terms of developing the dislocation theory of Granato–Lücke [3,5,6], it is assumed that the movement of dislocations detached from impurity atoms is limited not only by their linear tension, but also by the stress field of neighboring impurity atoms: dislocations detached from one impurity atom are fixed on other — neighboring ones. This mechanism limits the elongation of dislocation segments and the growth of the hysteresis loop area $\sigma = \sigma(\varepsilon)$. At small amplitudes of ε_m, this leads to a linear dependence of nonlinear losses on ε_m, and at large — to their saturation, at the same time, the unloading branches ($\varepsilon \geq 0$, $\dot{\varepsilon} < 0$ and $\varepsilon \leq 0$, $\dot{\varepsilon} > 0$) in hysteresis $\sigma = \sigma(\varepsilon)$ become nonlinear. No analytical dependences $\sigma = \sigma(\varepsilon)$ have been obtained in the works [14,27].

Note that, in contrast to ferromagnetic and ferroelectric hysteresis, easily observed on the oscilloscope [20]

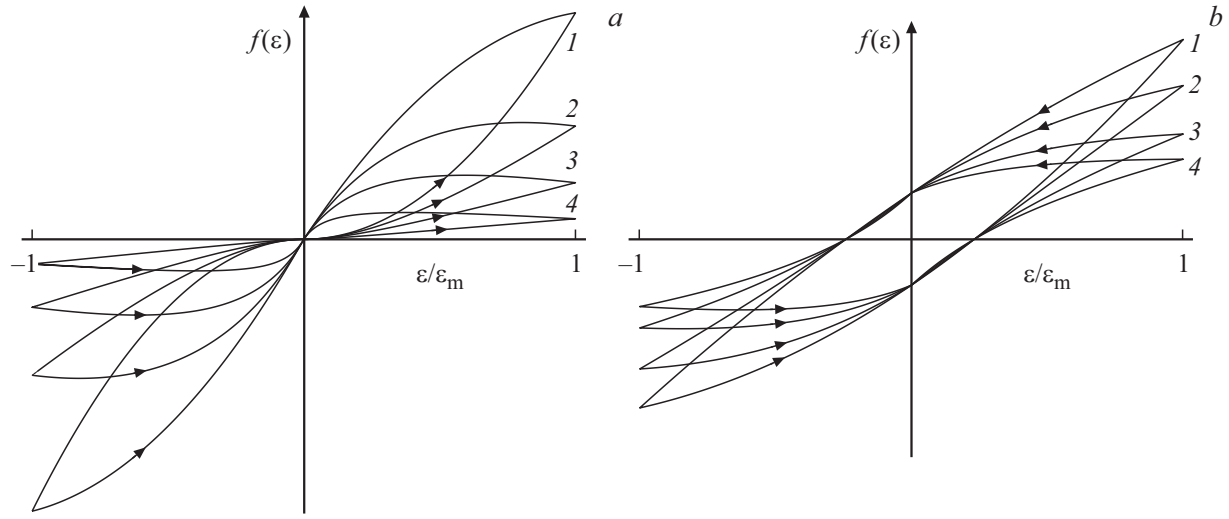

Figure 1. Qualitative view of elastic — (*a*) and inelastic — (*b*) hysteresis at different parameters γ_0 and $\alpha_{1,2}$: $\gamma_0 = 0$, $\alpha_{1,2} = 0{-}1$ and $\gamma_0 > 0$, $\alpha_{1,2} > 0$ — 2, 3, 4. Increasing the loop number corresponds to increasing the parameters γ_0 and $\alpha_{1,2}$.

screen, the similar observation „of mechanical" hysteresis is technically more difficult, although such hysteresis has certainly been observed [4,6]. This is because ferromagnetic and ferroelectric hysteresis are much more pronounced than „mechanical hysteresis": in the stress area, much smaller than the limit of elasticity of solids ($|\varepsilon| \ll |\varepsilon_{\text{th}}|$), the hysteresis nonlinearity is small: $|f(\varepsilon)| \ll |\varepsilon| \ll 1$. In this connection, mechanical hysteresis can be inferred from the patterns of NAEs in solids arising from the propagation of intense elastic waves in them. In this case, the hysteresis properties of the medium accumulate in the nonlinear distortion of the wave as it propagates and become quite visible to the measurement.

3. Network wave equation

When describing elastic waves in media with strong acoustic nonlinearity ($|f(\varepsilon)| \gg |\Gamma|\varepsilon^2$, Γ — the quadratic nonlinearity parameter of homogeneous media, $|\Gamma| < 10$), the geometric nonlinearity of equations of motion compared to physical nonlinearity of equation of state can be neglected. In this approximation, the equations of elasticity theory in Lagrangian and Eulerian forms coincide [24]. Substituting (1) into the equation of motion (in the Lagrangian form) $\rho U_{tt} = \sigma_x(\varepsilon)$, and considering the linear dissipation of the medium [28], we obtain a one-dimensional wave equation for the longitudinal (along the x axis) displacement $U = U(x, t)$

$$U_{tt} - C_0^2 U_{xx} = -C_0^2 \left[f(\varepsilon) - U_x^2/2 \right]_x + \eta U_{xxt}, \qquad (4)$$

where $C_0 = (E/\rho)^{1/2}$ — linear velocity of the longitudinal wave, η — linear dissipation factor, ρ — density, $\varepsilon(x, t) = U_x(x, t) + U_x^2(x, t)/2$, $\eta|U_{xxt}| \ll C_0^2|U_{xx}|$.

By differentiating equation (4) by x, and considering that $|f(\varepsilon)| \ll |\varepsilon| \ll 1$, $|f(\varepsilon)| \gg \varepsilon^2$, $\varepsilon \approx U_x$, we obtain equation for longitudinal strain $\varepsilon = \varepsilon(x, t)$

$$\varepsilon_{tt} - C_0^2 \varepsilon_{xx} = -C_0^2 [f(\varepsilon)]_{xx} + \eta \varepsilon_{xxt}. \qquad (5)$$

Turning in equation (5) to the accompanying coordinate system $\tau = t - x/C_0$, $x' = x \geq 0$, we obtain a nonlinear evolution equation for waves running in the positive direction of axis x:

$$\frac{\partial \varepsilon}{\partial x} = -\frac{1}{2C_0} \frac{\partial f(\varepsilon)}{\partial \tau} + \frac{\eta}{2C_0^3} \frac{\partial^2 \varepsilon}{\partial \tau^2}. \qquad (6)$$

A similar wave equation holds for the velocity $V(x, \tau) = U_\tau(x, \tau)$ of the particles in the medium, since for travelling waves the following relation holds: $\varepsilon(x, \tau) = -V(x, \tau)/C_0$.

To investigate the nonlinear acoustic effects occurring during propagation in a polycrystal IHW, we solve equation (6) with the perturbation method. The boundary condition is given as a harmonic oscillation: $\varepsilon(x = 0, t) = \varepsilon_0 \sin \omega t$, where ε_0 and ω — the amplitude of strain and frequency of oscillation produced by the emitter.

Assuming in the equations (6), that

$$\varepsilon(x, \theta) = \sum_{n=1}^{\infty} \bar{\varepsilon}_n(x, \theta) = \sum_{n=1}^{\infty} \varepsilon_n(\varepsilon_0, x) \sin[n\theta + \psi_n(\varepsilon_0, x)],$$

$$\left| \sum_{n=2}^{\infty} \bar{\varepsilon}_n(x, \theta) \right| \ll |\bar{\varepsilon}_1(x, \theta)|,$$

$$\varepsilon_1(\varepsilon_0, x) \approx \varepsilon_m(\varepsilon_0, x), \quad \varepsilon_{n\geq 2}(x = 0) = 0,$$

we get the equation for the amplitudes $\varepsilon_n(\varepsilon_0, x)$ and phases $\Phi(\varepsilon_0, x)$, $\psi_n(\varepsilon_0, x)$:

$$\left(\frac{d\varepsilon_n}{dx} + \frac{\eta K_n^2}{2C_0} \varepsilon_n \right) \begin{pmatrix} \cos\psi_n \\ \sin\psi_n \end{pmatrix} \mp \varepsilon_n \left(n \frac{d\Phi}{dx} + \frac{d\psi_n}{dx} \right) \times \begin{pmatrix} \sin\psi_n \\ \cos\psi_n \end{pmatrix} = \pm \frac{K_n}{2} \begin{pmatrix} a_n(\varepsilon_1) \\ b_n(\varepsilon_1) \end{pmatrix}, \qquad (7)$$

where

$$\begin{pmatrix} a_n(\varepsilon_1) \\ b_n(\varepsilon_1) \end{pmatrix} = \frac{1}{\pi}\int\limits_0^{2\pi} f\left[\bar{\varepsilon}_1(x,\theta)\right]\begin{pmatrix} \cos n\theta \\ \sin n\theta \end{pmatrix} d\theta,$$

$$K_n = nK_1 = n\omega/C_0,\ \ \theta = \omega\tau + \Phi(x),\ \ \psi_1(x) = 0.$$

The derivatives $\Phi_x(\varepsilon_0, x)$ and $\psi_{nx}(\varepsilon_0, x)$ determine the local changes in the phase velocities $C_1(\varepsilon_0, x)$ and $C_n(\varepsilon_0, x)$ of the primary wave and its harmonics:

$$\xi(\varepsilon_0, x) = \frac{C_1(\varepsilon_0, x) - C_0}{C_0} = \frac{1}{K_1}\frac{d\Phi(\varepsilon_0, x)}{dx},$$

$$\xi_n(\varepsilon_0, x) = \frac{C_n(\varepsilon_0, x) - C_1(\varepsilon_0, x)}{C_0} = \frac{1}{nK_1}\frac{d\psi_n(\varepsilon_0, x)}{dx}.$$

It follows from the last expression that if $\xi_n(\varepsilon_0, x) \neq 0$, then $C_n(\varepsilon_0, x) \neq C_1(\varepsilon_0, x)$, i.e. the medium has a nonlinear phase velocity dispersion. Let us determine the effective (average) nonlinear decrement of decay $\delta(\varepsilon_0)$ and the relative change in phase velocity $\xi(\varepsilon_0)$ of the primary wave at distance x from the emitter

$$\delta(\varepsilon_0) = -2\pi\left(\frac{\ln[\varepsilon_1(x)/\varepsilon_0]}{K_1 x} + \frac{\eta\omega}{2C_0^2}\right),$$

$$\xi(\varepsilon_0) = \frac{1}{K_1 x}\int\limits_0^x \xi(\varepsilon_0, x')dx' = \frac{\Phi(\varepsilon_0, x)}{K_1 x}. \qquad (8)$$

3.1. NAE in media with elastic hysteresis

For elastic hysteresis (2), equations (7) for the amplitudes and phases of the first three harmonics have the form

$$\frac{d\varepsilon_1}{dz} + g\varepsilon_1 = -\frac{1}{2\gamma_0^2}\left(1 + \frac{\gamma_0\varepsilon_1}{2} - \frac{(1+\gamma_0\varepsilon_1)\ln(1+\gamma_0\varepsilon_1)}{\gamma_0\varepsilon_1}\right),$$

$$\frac{d\Phi}{dz} = \frac{1}{2\gamma_0^2\varepsilon_1}\left(1 - \frac{b}{\gamma_0\varepsilon_1}\right) \times \left(\frac{\pi}{2} - \gamma_0\varepsilon_1 - \frac{\ln\left[\gamma_0\varepsilon_1 + \sqrt{(\gamma_0\varepsilon_1)^2 - 1}\right]}{\sqrt{(\gamma_0\varepsilon_1)^2 - 1}}\right) - \frac{\pi b}{8\gamma_0},$$

$$\left(\frac{d\varepsilon_2}{dz} + 4g\varepsilon_2\right)\cos\psi_2 - \varepsilon_2\left(2\frac{d\Phi}{dz} + \frac{d\psi_2}{dz}\right)\sin\psi_2 = -\frac{c\varepsilon_1}{3\gamma_0}\left\{1 - \frac{6}{\gamma_0\varepsilon_1}\left(\frac{d}{c} - \frac{1}{\gamma_0\varepsilon_1}\right)\left(1 - \frac{\pi}{2\gamma_0\varepsilon_1} + \frac{[2-(\gamma_0\varepsilon_1)^2]\ln\left[\gamma_0\varepsilon_1 + \sqrt{(\gamma_0\varepsilon_1)^2-1}\right]}{2\gamma_0\varepsilon_1\sqrt{(\gamma_0\varepsilon_1)^2-1}}\right)\right\},$$

$$\left(\frac{d\varepsilon_2}{dz} + 4g\varepsilon_2\right)\sin\psi_2 + \varepsilon_2\left(2\frac{d\Phi}{dz} + \frac{d\psi_2}{dz}\right)\cos\psi_2 = \frac{d\varepsilon_1}{3\gamma_0}\left(1 - \frac{3}{\gamma_0\varepsilon} - \frac{6}{(\gamma_0\varepsilon_1)^2} + \frac{6(1+\gamma_0\varepsilon_1)\ln(1+\gamma_0\varepsilon_1)}{(\gamma_0\varepsilon_1)^3}\right), \qquad (9)$$

$$\left(\frac{d\varepsilon_3}{dz} + 9g\varepsilon_3\right)\cos\psi_3 - \varepsilon_3\left(3\frac{d\Phi}{dz} + \frac{d\psi_3}{dz}\right)\sin\psi_3 = -\frac{\varepsilon_1}{4\gamma_0}\left(1 + \frac{10}{\gamma_0\varepsilon_1} - \frac{12}{(\gamma_0\varepsilon_1)^2} - \frac{24}{(\gamma_0\varepsilon_1)^3} + \frac{6(1+\gamma_0\varepsilon_1)[4-(\gamma_0\varepsilon_1)^2]\ln(1+\gamma_0\varepsilon_1)}{(\gamma_0\varepsilon_1)^4}\right),$$

$$\left(\frac{d\varepsilon_3}{dz} + 9g\varepsilon_3\right)\sin\psi_3 + \varepsilon_3\left(3\frac{d\Phi}{dz} + \frac{d\psi_3}{dz}\right)\cos\psi_3 = -\frac{\varepsilon_1}{2\gamma_0}\left(1 - \frac{b}{\gamma_0\varepsilon_1}\right)\left(1 - \frac{3\pi}{2\gamma_0\varepsilon_1} - \frac{12}{(\gamma_0\varepsilon_1)^2} + \frac{6\pi}{(\gamma_0\varepsilon_1)^3} - \frac{3[4-3(\gamma_0\varepsilon_1)^2]\ln\left[\gamma_0\varepsilon_1 + \sqrt{(\gamma_0\varepsilon_1)^2-1}\right]}{(\gamma_0\varepsilon_1)^3\sqrt{(\gamma_0\varepsilon_1)^2-1}}\right),$$

where $z = aK_1x$,

$$a = \frac{\gamma_1+\gamma_2+\gamma_3+\gamma_4}{2\pi}, \quad b = \frac{\gamma_1-\gamma_2+\gamma_3-\gamma_4}{\gamma_1+\gamma_2+\gamma_3+\gamma_4},$$

$$c = \frac{\gamma_1-\gamma_2-\gamma_3+\gamma_4}{\gamma_1+\gamma_2+\gamma_3+\gamma_4}, \quad d = \frac{\gamma_1+\gamma_2-\gamma_3-\gamma_4}{\gamma_1+\gamma_2+\gamma_3+\gamma_4},$$

$$g = \frac{\pi\eta\omega}{(\gamma_1+\gamma_2+\gamma_3+\gamma_4)C_0^2}, \quad gz = \frac{\eta\omega^2 x}{2C_0^3}.$$

In the general case, analytical solutions of equations (9) cannot be obtained, so we consider two simple limiting cases, and then give the results of numerical solutions of these equations.

In low-amplitude mode ($\gamma_0\varepsilon_0 \ll 1$), at $gz \ll 1$ and $\varepsilon_0 z \ll 1$, we get

$$\varepsilon_1(\varepsilon_0) = \frac{\varepsilon_0\exp(-gz)}{1+\varepsilon_0 z/12}, \quad \Phi(\varepsilon_0) = -b_1\varepsilon_0 z,$$

$$\delta(\varepsilon_0) = \frac{\pi a\varepsilon_0}{6}, \quad \xi(\varepsilon_0) = -ab_1\varepsilon_0,$$

$$r(\varepsilon_0) = \frac{\delta(\varepsilon_0)}{|\xi(\varepsilon_0)|} = \frac{\pi}{6b_1} = \text{const}, \qquad (10)$$

$$\varepsilon_2(\varepsilon_0) = \sqrt{a_2^2+b_2^2}\,\varepsilon_0^2 z, \quad \varepsilon_3(\varepsilon_0) = \sqrt{a_3^2+b_3^2}\,\varepsilon_0^2 z,$$

$$\operatorname{tg}\psi_n = -a_n/b_n,$$

where

$$b_1 = \pi/8 + b/3, \quad a_2 = \pi c/8 + d/3, \quad b_2 = -d/6,$$

$$a_3 = 1/20, \quad b_3 = -b/5.$$

In saturation mode ($\gamma_0\varepsilon_0 \gg 1$) at $gz \ll 1$, we get

$$\varepsilon_1(\varepsilon_0) = \varepsilon_0\exp\left[-\left(g + \frac{1}{4\gamma_0}\right)z\right],$$

$$\Phi(\varepsilon_0) = -\frac{z}{2\gamma_0}\left(1 + \frac{\pi b}{4}\right),$$

$$\delta(\varepsilon_0) = \frac{\pi a}{2\gamma_0}, \quad \xi(\varepsilon_0) = -\frac{a}{2\gamma_0}\left(1 + \frac{\pi b}{4}\right),$$

$$r(\varepsilon_0)=\frac{\delta(\varepsilon_0)}{|\xi(\varepsilon_0)|}=\frac{\pi}{1+\pi b/4}=\text{const},$$

$$\varepsilon_2(\varepsilon_0)=\frac{\sqrt{c^2+d^2}\varepsilon_0 z}{3\gamma_0},$$

$$\psi_2(\varepsilon_0)=\frac{\pi}{2}+\operatorname{arctg}\left(\frac{c}{d}\right)+\frac{z}{\gamma_0}\left(1+\frac{\pi b}{4}\right),$$

$$\varepsilon_3(\varepsilon_0)=\frac{\sqrt{5}\varepsilon_0 z}{4\gamma_0},$$

$$\psi_3(\varepsilon_0)=\frac{\pi}{2}-\operatorname{arctg}\left(\frac{1}{2}\right)+\frac{3z}{2\gamma_0}\left(1+\frac{\pi b}{4}\right). \qquad (11)$$

3.2. NAE in media with inelastic hysteresis

Similarly, for inelastic hysteresis (3), equations (7) for the amplitudes and phases of the first three harmonics have the form

$$\frac{d\varepsilon_1}{dz}+g\varepsilon_1=-\frac{1}{\alpha_2^2}\left(1-\frac{\alpha_2\varepsilon_1}{2}-\frac{[1-(\alpha_2\varepsilon_1)^2]\ln(1+\alpha_2\varepsilon_1)}{\alpha_2\varepsilon_1}\right),$$

$$\frac{d\Phi}{dz}=\frac{4b}{\alpha_1^2\varepsilon_1}\left[\frac{\pi}{2}-\alpha_1\varepsilon_1-\frac{2}{\sqrt{1-(\alpha_1\varepsilon_1)^2}}\operatorname{arctg}\left(\sqrt{\frac{1-\alpha_1\varepsilon_1}{1+\alpha_1\varepsilon_1}}\right)\right],$$

$$\left(\frac{d\varepsilon_2}{dz}+4g\varepsilon_2\right)\cos\psi_2-\varepsilon_2\left(2\frac{d\Phi}{dz}+\frac{d\psi_2}{dz}\right)\sin\psi_2$$

$$=-\frac{c\varepsilon_1}{3\gamma_0}\left\{1-\frac{6}{2\gamma_0\varepsilon_1}\left(\frac{d}{c}-\frac{1}{\gamma_0\varepsilon_1}\right)\right.$$

$$\left.\times\left(1-\frac{\pi}{2\gamma_0\varepsilon_1}+\frac{[2-(\gamma_0\varepsilon_1)^2]\ln\left[\gamma_0\varepsilon_1+\sqrt{(\gamma_0\varepsilon_1)^2-1}\right]}{2\gamma_0\varepsilon_1\sqrt{(\gamma_0\varepsilon_1)^2-1}}\right)\right\},$$

$$\left(\frac{d\varepsilon_2}{dz}+4g\varepsilon_2\right)\sin\psi_2+\varepsilon_2\left(2\frac{d\Phi}{dz}+\frac{d\psi_2}{dz}\right)\cos\psi_2=0,$$

$$\left(\frac{d\varepsilon_3}{dz}+9g\varepsilon_3\right)\cos\psi_3-\varepsilon_3\left(3\frac{d\Phi}{dz}+\frac{d\psi_3}{dz}\right)\sin\psi_3$$

$$=\frac{9\varepsilon_1}{2\alpha_2}\left(1-\frac{22}{9\alpha_2\varepsilon_1}-\frac{4}{3(\alpha_2\varepsilon_1)^2}+\frac{16}{3(\alpha_2\varepsilon_1)^3}\right.$$

$$\left.-\frac{2[1-(\alpha_2\varepsilon_1)^2][4-(\alpha_2\varepsilon_1)^2]\ln(1+\alpha_2\varepsilon_1)}{3(\alpha_2\varepsilon_1)^4}\right),$$

$$\left(\frac{d\varepsilon_3}{dz}+9g\varepsilon_3\right)\sin\psi_3+\varepsilon_3\left(3\frac{d\Phi}{dz}+\frac{d\psi_3}{dz}\right)\cos\psi_3$$

$$=-\frac{4b\varepsilon_1}{\alpha_1}\left[1-\frac{3\pi}{2\alpha_1\varepsilon_1}-\frac{12}{(\alpha_1\varepsilon_1)^2}+\frac{6\pi}{(\alpha_1\varepsilon_1)^3}\right.$$

$$\left.-\frac{6[4-3(\alpha_1\varepsilon_1)^2]}{(\alpha_1\varepsilon_1)^3\sqrt{1-(\alpha_1\varepsilon_1)^2}}\operatorname{arctg}\left(\sqrt{\frac{1-\alpha_1\varepsilon_1}{1+\alpha_1\varepsilon_1}}\right)\right], \qquad (12)$$

where

$$z=aK_1x,\quad a=\frac{\beta_1+\beta_2}{2\pi},\quad g=\frac{\pi\eta\omega}{(\beta_1+\beta_2)C_0^2},$$

$$b=\frac{\beta}{\beta_1+\beta_2},\quad c=\frac{\beta_1-\beta_2}{\beta_1+\beta_2},\quad gz=\frac{\eta\omega^2x}{2C_0^3}.$$

In the low-amplitude mode ($\alpha_{1,2}\varepsilon_0\ll 1$) at $gz\ll 1$ and $\varepsilon_0 z\ll 1$, we get

$$\varepsilon_1(\varepsilon_0)=\frac{\varepsilon_0\exp(-gz)}{1+(2\varepsilon_0 z/3)},\quad \Phi(\varepsilon_0)=-\pi b\varepsilon_0 z,$$

$$\delta(\varepsilon_0)=\frac{4\pi a\varepsilon_0}{3},\quad \xi(\varepsilon_0)=-\pi ab\varepsilon_0,$$

$$r(\varepsilon_0)=\frac{\delta(\varepsilon_0)}{|\xi(\varepsilon_0)|}=\frac{4}{3b}=\text{const},$$

$$\varepsilon_2(\varepsilon_0)=-\frac{\pi c\varepsilon_0^2 z}{4},\quad \psi_2(\varepsilon_0)=\pi b\varepsilon_0 z,$$

$$\varepsilon_3(\varepsilon_0)=-\frac{2\varepsilon_0^2 z}{5},\quad \psi_3(\varepsilon_0)=\frac{3\pi b\varepsilon_0 z}{2}. \qquad (13)$$

In saturation mode ($\alpha_{1,2}\varepsilon_0\gg 1$) at $gz\ll 1$ and $[\ln(\alpha_2\varepsilon_0)/\alpha_2]z\ll 1$ we get

$$\varepsilon_1(\varepsilon_0)=\varepsilon_0\exp\left[-\left(g+\frac{\ln(\alpha_2\varepsilon_0)}{\alpha_2}\right)z\right]=\varepsilon_0^{n(z)}\alpha_2^{-z/\alpha_2}\exp(-gz),$$

$$\Phi(\varepsilon_0)=-\frac{4bz}{\alpha_1},$$

$$\delta(\varepsilon_0)=2\pi a\frac{\ln(\alpha_2\varepsilon_0)}{\alpha_2},\quad \xi(\varepsilon_0)=-\frac{4ab}{\alpha_1},$$

$$r(\varepsilon_0)=\frac{\delta(\varepsilon_0)}{|\xi(\varepsilon_0)|}=\frac{\pi\alpha_1\ln(\alpha_2\varepsilon_0)}{2\alpha_2 b}\neq\text{const},$$

$$\varepsilon_2(\varepsilon_0)=-\frac{2c\varepsilon_0 z}{3\alpha_2},\quad \psi_2(\varepsilon_0)=\frac{4bz}{\alpha_1},$$

$$\varepsilon_3(\varepsilon_0)=-4\varepsilon_0 z\left[\left(\frac{b}{\alpha_1}\right)^2+\left(\frac{3\ln(\alpha_2\varepsilon_0)}{4\alpha_2}\right)^2\right]^{1/2},$$

$$\psi_3(\varepsilon_0)=\frac{6b}{\alpha_1}\left(z+\frac{2\alpha_2}{9\ln(\alpha_2\varepsilon_0)}\right), \qquad (14)$$

where $n(z)=1-z/\alpha_2<1$.

It follows from expressions (10), (13) that in the low-amplitude regime (at $z=\text{const}$), the amplitude dependence of the NAE for media with elastic and inelastic hysteresis is the same: $\delta(\varepsilon_0)\propto\varepsilon_0$, $\xi(\varepsilon_0)\propto\varepsilon_0$, $\varepsilon_{2,3}(\varepsilon_0)\propto\varepsilon_0^2$. In this mode, the independent characteristics of the nonlinear wave are $\delta(\varepsilon_0)$, $\xi(\varepsilon_0)$ and $\varepsilon_2(\varepsilon_0)$, and $\varepsilon_3(\varepsilon_0)$ can be calculated from the measured values of $\delta(\varepsilon_0)$ and $\xi(\varepsilon_0)$. Thus, from the comparison and correspondence (or mismatch) between the calculated (for the elastic and inelastic hysteresis) and the experimentally measured amplitude $\varepsilon_3(\varepsilon_0)$ it can be determined which hysteresis determines the ADIF effects in the polycrystal studied. In the saturation mode, however, the amplitude dependences $\xi(\varepsilon_0)$ and $\varepsilon_2(\varepsilon_0)$ for different hysteresis are the same [$\xi(\varepsilon_0)=\text{const}$, $\varepsilon_2(\varepsilon_0)\propto\varepsilon_0$], but $\delta(\varepsilon_0)$ and $\varepsilon_3(\varepsilon_0)$ — are different, while for elastic

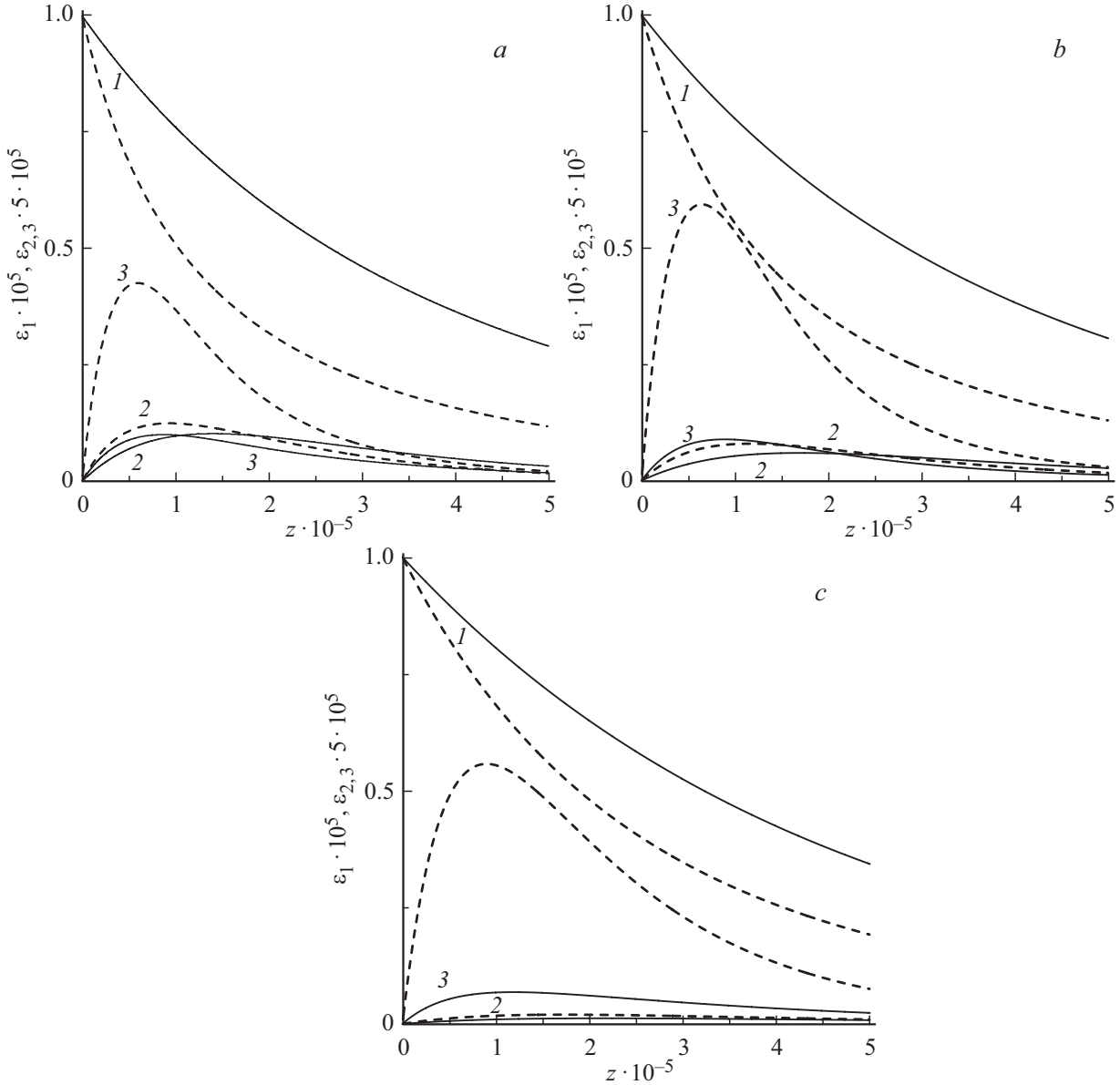

Figure 2. Dependences of amplitudes ε_1 — 1, ε_2 — 2, ε_3 — 3 on z when $\varepsilon_0 = 10^{-5}$, $g = 2 \cdot 10^{-6}$, $b = 1/5$, $c = 1/10$, $d = 0$ and different values of γ_0 and $\alpha_1 = \alpha_2$: $\gamma_0, \alpha_{1,2} = 0$ — *a*, $\gamma_0, \alpha_{1,2} = 10^5$ — *b*, $\gamma_0, \alpha_{1,2} = 10^6$ — *c*. Solid lines — for elastic hysteresis, dashed lines — for inelastic hysteresis.

hysteresis — $\delta(\varepsilon_0) = \text{const}$, $\varepsilon_3(\varepsilon_0) \propto \varepsilon_0$, and for inelastic — $\delta(\varepsilon_0) \propto \ln(\alpha_2\varepsilon_0) \neq \text{const}$,

$$\varepsilon_3(\varepsilon_0) \propto \varepsilon_0 \left[\left(\frac{b}{\alpha_1} \right)^2 + \left(\frac{3\ln(\alpha_2\varepsilon_0)}{4\alpha_2} \right)^2 \right]^{1/2}.$$

Here is the answer to the question which hysteresis (elastic or inelastic) is determined by ADIF effects in the studied polycrystal can be obtained, firstly, from the correspondence between the amplitude dependences of the NAE established in the experiment and the analytical ones (11), (14), and, secondly, from a comparison of the saturation parameters γ_0 and $\alpha_{1,2}$ determined from the dependences $\delta(\varepsilon_0)$, $\xi(\varepsilon_0)$ and $\varepsilon_{2,3}(\varepsilon_0)$ on ε_0.

4. Results of the numerical counting

Expressions (10)–(14) determine the patterns of NAE in solids with elastic (2) and inelastic (3) hysteresis in the limiting regimes: without saturation and with ADIF saturation. A more complete picture of the behavior of the NAE (at specific hysteresis parameters) is given by the results of numerical solutions of equations (9), (12). Fig. 2 shows the dependences of $\varepsilon_{1,2,3}(\varepsilon_0)$ on z when $\varepsilon_0 = 10^{-5}$, $g = 2 \cdot 10^{-6}$, $b = 1/5$, $c = 1/10$, $d = 0$, $\gamma_1 + \gamma_2 + \gamma_3 + \gamma_4 = \beta_1 + \beta_2$ and different parameter values γ_0 and $\alpha_1 = \alpha_2$. Figure 2 shows that as z increases, the amplitude of ε_1 of the first harmonic decreases monotonically (due to linear and hysteresis losses), while the amplitude of ε_1 decreases more slowly in a

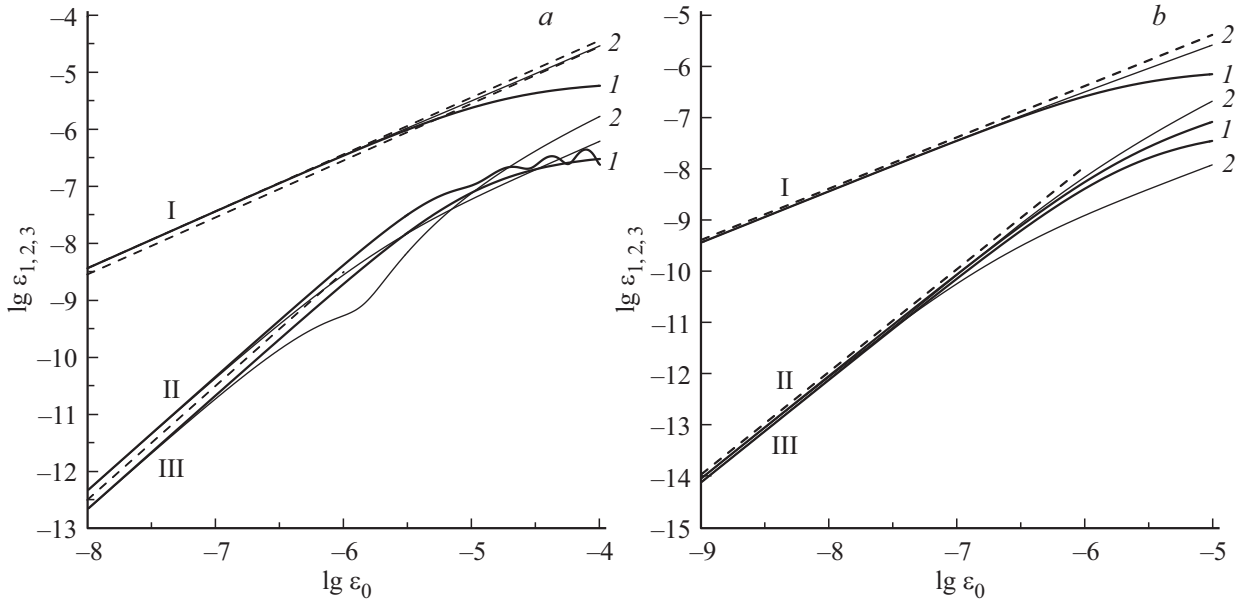

Figure 3. *a* — dependences of ε_1 — I, ε_2 — II and ε_3 — III on ε_0 at $z = 10^6$, $g = 10^{-6}$, $b = 1/2$, $c = 1/5$, $d = 0$ and different parameter values γ_0: $\gamma_0 = 0$ — *1* and $\gamma_0 = 10^6$ — *2*. The dotted lines correspond to the dependences: I — $\varepsilon_1 \propto \varepsilon_0$, II, III — $\varepsilon_{2,3} \propto \varepsilon_0^2$; *b* — dependences of ε_1 — I, ε_2 — II and ε_3 — III on ε_0 at $z = 10^6$, $g = 10^{-6}$, $b = 1/2$, $c = 1/5$ and different parameter values $\alpha_1 = \alpha_2$: $\alpha_{1,2}$ — *1* and $\alpha_{1,2} = 10^7$ — *2*. The dotted lines correspond to the dependences: I — $\varepsilon_1 \propto \varepsilon_0$, II, III — $\varepsilon_{2,3} \propto \varepsilon_0^2$.

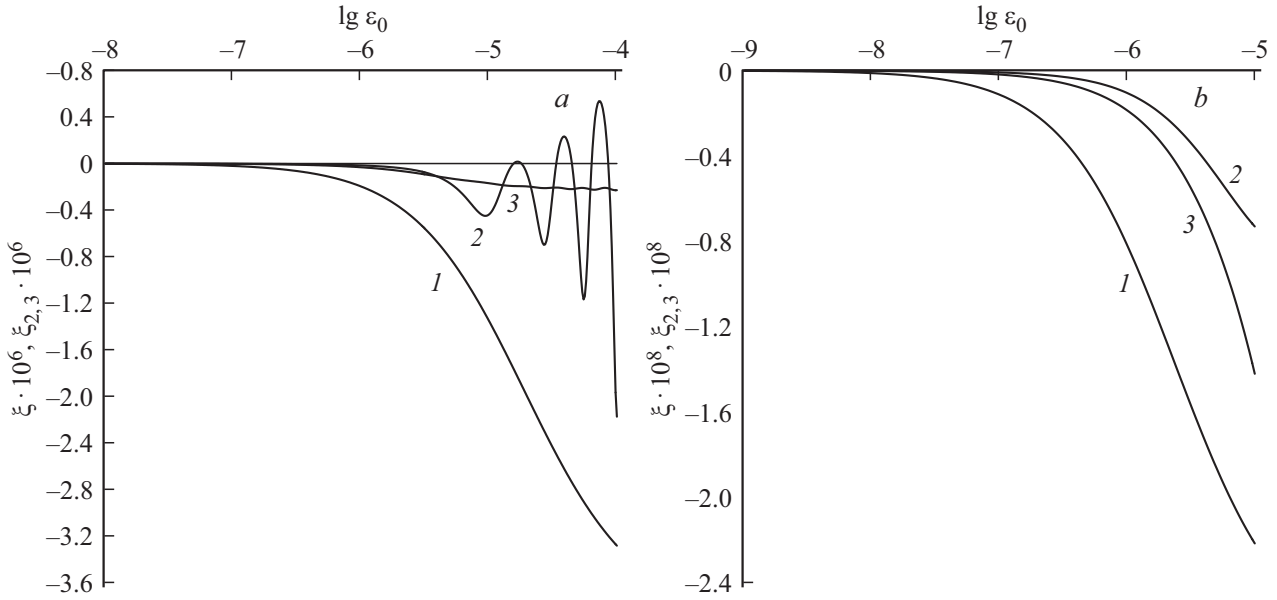

Figure 4. *a* — dependences of $\xi(\varepsilon_0, z)$ — lines *1* and $\xi_{2,3}(\varepsilon_0, z)$ — lines *2, 3* from ε_0 for elastic hysteresis at $\gamma_0 = 0$, $z = 10^6$, $b = 1/2$, $c = 1/5$, $d = 0$; *b* — dependences $\xi(\varepsilon_0, z)$ — lines *1* and $\xi_{2,3}(\varepsilon_0, z)$ — lines *2, 3* on ε_0 for inelastic hysteresis at $\alpha_{1,2} = 0$, $z = 10^6$, $b = 1/2$, $c = 1/5$, $d = 0$.

medium with elastic hysteresis than with inelastic hysteresis. When the parameters γ_0 and α_2 are increased (due to reduced hysteresis losses), the amplitude of ε_1 decreases more slowly. With increase z the amplitudes of $\varepsilon_{2,3}$ first increase, reach a maximum and then decrease, with γ_0 and $\alpha_{1,2}$ increasing, the amplitude of ε_2 decreases and ε_3 changes non-monotonically. It should also be noted that the amplitudes of $\varepsilon_{2,3}$ in a medium with inelastic hysteresis are noticeably higher than in a medium with elastic hysteresis.

More interesting and informative nonlinear wave characteristic dependences are those of $\varepsilon_{1,2,3}(\varepsilon_0)$ on ε_0 (at $z = \text{const}$), since in a solid it is difficult to change receiver location (coordinate z, i.e. x), but one can easily change amplitude of ε_0. In Fig. 3, *a, b* — for elastic (*a*) and inelastic (*b*) hysteresis, the $\varepsilon_{1,2,3}(\varepsilon_0)$ dependence on ε_0

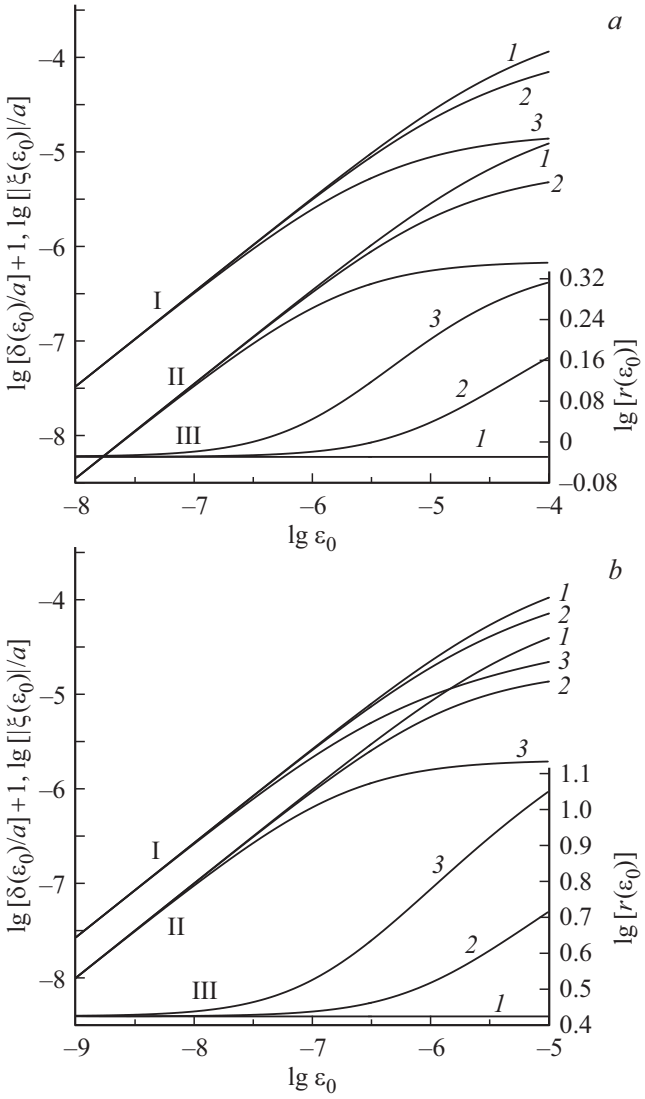

Figure 5. *a* — dependency plots $\delta(\varepsilon_0)/a$ — I, $\xi(\varepsilon_0)/a$ — II and $r(\varepsilon_0) = \delta(\varepsilon_0/|\xi(\varepsilon_0)|)$ — III on ε_0 for elastic hysteresis at $z = 10^6$, $g = 10^{-6}$, $b = 1/2$ and different values of parameter γ_0: $\gamma_0 = 0$ — *1*, $\gamma_0 = 10^5$ — *2*, $\gamma_0 = 10^6$ — *3*; *b* — dependency plots $\delta(\varepsilon_0)/a$ — I, $\xi(\varepsilon_0)/a$ — II and $r(\varepsilon_0) = \delta(\varepsilon_0/|\xi(\varepsilon_0)|)$ — III of ε_0 for inelastic hysteresis at $z = 10^6$, $g = 10^{-6}$, $b = 1/2$ and different parameter values $\alpha_1 = \alpha_2$: $\alpha_{1,2} = 0$ — *1*, $\alpha_{1,2} = 10^6$ — *2*, $\alpha_{1,2} = 10^7$ — *3*.

(at $z = 10^6$) is shown. Fig. 3, *a, b* shows that with $\gamma_0 = 0$, $\alpha_{1,2} = 0$ as ε_0 increases, first — $\varepsilon_1 \propto \varepsilon_0$, $\varepsilon_{2,3} \propto \varepsilon_0^2$, and then — $\varepsilon_{1,2,3}$ tend to saturate. Small amplitude oscillations of $\varepsilon_{2,3}(\varepsilon_0)$ (Fig. 3, *a*, $\gamma_0 = 0$) are related with the appearance of nonlinear dispersion of the wave phase velocity in a medium with elastic hysteresis. At $\gamma_0 \neq 0$, as ε_0 grows, at $\gamma_0\varepsilon_0 \ll 1$ — $\varepsilon_1 \propto \varepsilon_0$ $\varepsilon_{2,3} \propto \varepsilon_0^2$, and at $\alpha_{1,2}\varepsilon_0 \gg 1$ — $\varepsilon_{1,2,3} \propto \varepsilon_0$. At $\alpha_{1,2} \neq 0$, at $\alpha_{1,2}\varepsilon_0 \ll 1$ — $\varepsilon_1 \propto \varepsilon_0$, $\varepsilon_{2,3} \propto \varepsilon_0^2$, and at $\alpha_{1,2}\varepsilon_0 \gg 1$ — $\varepsilon_1 \propto \varepsilon_0^{n(z)}$, where $n(z) = 1 - z/\alpha_2 = 0.9$, and the dependences of $\varepsilon_{2,3}$ on ε_0 are close to linear.

In Fig. 4, *a, b* — for the elastic (*a*) and inelastic (*b*) hysteresis, plots of the dependence $\xi(\varepsilon_0, z)$ and $\xi_{2,3}(\varepsilon_0, z)$ from ε_0 at $\gamma_0 = 0$, $\alpha_{1,2} = 0$, $z = 10^6$, $b = 1/2$, $c = 1/5$, $d = 0$. These figures show that (at $\varepsilon_0 = \text{const}$) the values of $\xi(\varepsilon_0, z)$ and $\xi_{2,3}(\varepsilon_0, z)$ for the elastic hysteresis are significantly higher than those for the inelastic hysteresis, while for $\xi_2(\varepsilon_0, z)$ in the range $10^{-5} < \varepsilon_0 < 10^{-4}$ oscillations are observed. Thus, the nonlinear dispersion (phase velocity) for the medium with elastic hysteresis is much larger than the nonlinear dispersion for the medium with inelastic hysteresis, which appears in the oscillation of the amplitudes $\varepsilon_{2,3}$ in Fig. 3, *a* (for elastic hysteresis at $\gamma_0 = 0$) and its absence in Fig. 3, *b* (for inelastic hysteresis).

In Fig. 5, *a, b* — for elastic (*a*) and inelastic (*b*) hysteresis, plots of $\delta(\varepsilon_0)/a$ are shown, $\xi(\varepsilon_0)/a$ and $r(\varepsilon_0) = \delta(\varepsilon_0)/||\xi(\varepsilon_0)|$ on ε_0 at $z = 10^6$, $g = 10^{-6}$, $b = 1/2$ and different parameter values γ_0 and $\alpha_{1,2}$.

Figure 5 shows that in the low-amplitude regime ($\gamma_0\varepsilon_0 \ll 1$, $\alpha_{1,2}\varepsilon_0 \ll 1$), the dependences $\delta = \delta(\varepsilon_0)$ and $\xi = \xi(\varepsilon_0)$ for the elastic and inelastic hysteresis are the same: $\delta(\varepsilon_0) \propto \varepsilon_0$, $\xi(\varepsilon_0) \propto \varepsilon_0$, $r(\varepsilon_0) = \text{const}$. In saturation mode ($\gamma_0\varepsilon_0 \gg 1$, $\alpha_{1,2}\varepsilon_0 \gg 1$) these dependences are different for different hysteresis. For elastic hysteresis: $\delta(\varepsilon_0) \to \text{const}$, $\xi(\varepsilon_0) \to \text{const}$, $r(\varepsilon_0) \to \text{const}$ and for inelastic $\delta(\varepsilon_0) \propto \ln(\alpha_1)\varepsilon_0$, $\xi(\varepsilon_0) \to \text{const}$, $r(\varepsilon_0) \propto \ln(\alpha_2\varepsilon_0) \neq \text{const}$. This difference in the behavior of $\delta(\varepsilon_0)$, $\xi(\varepsilon_0)$ and $r(\varepsilon_0)$ is also a distinctive feature of the elastic and inelastic hysteresis behavior in the saturation ADIF regime.

5. Conclusion

In this paper, theoretical and numerical studies of NAEs arising from the propagation of initially harmonic waves in visco-elastic hysteresis solids with ADIF saturation have been carried out. Two main types of quadratic hysteresis are considered: elastic (or breakaway hysteresis) and inelastic (or microplastic hysteresis). The method of perturbation determines patterns of NAE in such media in low-amplitude and saturation modes: nonlinear losses and changes of primary wave propagation velocity, as well as amplitudes and phases of its second and third harmonics. A comparative analysis of the patterns of nonlinear effects has been carried out and a method for determining the hysteresis type has been proposed, based on the analysis and correspondence of the obtained analytical and experimentally determined amplitude dependences and NAE levels in such media. The experimental determination of the amplitude dependences of NAE for hysteresis solids and their comparison with theoretical ones — for media with different hysteresis (elastic and inelastic) will contribute to a correct choice of hysteresis equations of state for such media and to identification of physical mechanisms of their hysteresis nonlinearity.

Financial support of work

The work has been performed under the state assignment of IAP RAS institute of Applied Physics on the topic

No.0030-2021-0009 and supported by the Russian Foundation for Basic Research (Grant N20-02-00215A).

Conflict of interest

The authors declare that they have no conflict of interest.

References

[1] N.N. Davidenkov. ZhTF **8**, *6*, 483 (1938).
[2] T.A. Read. Phys. Rev. **58**, 371 (1940).
[3] A. Granato, K. Lucke. J. Appl. Phys. **27**, *7*, 789 (1956).
[4] Dislocations and Mechanical Properties of Crystals / Translated from English, ed. M.V. Klassen-Nekludova, V.L. Indenbom. IL, M. (1960). 552 p. (in Russian).
[5] Ultrasonic methods of studying dislocations. Coll. articles / Translated from English and German, ed. L.G. Merkulova. IL, M. (1963). 376 p. (in Russian).
[6] Physical acoustics / Ed. W. Mezon. Mir, M. (1969). V. 4. P. A. 375 p. (in Russian).
[7] D.H. Niblett, J. Wilks. UFN **80**, 125 (1963).
[8] S.P. Nikanorov, B.K. Kardashev. Elasticity and dislocation inelasticity of crystals. Nauka, M. (1985). 250 p. (in Russian).
[9] V.P. Levin, V.B. Proskurin, Dislocation inelasticity in metals. Nauka, M. (1993). 272 p.
[10] P.P. Pal-Val, V.D. Natsik, L.N. Pal-Val, Yu.A. Semerenko. Low Temperature Physics **30**, *1*, 115 (2004).
[11] M.S. Blanter, I.S. Golovin, H. Neuhauser, H.-R. Sunning. Internal Friction in Metallic Materials. A Handbook. Springer-Verlag, Berlin–Heidelberg (2007). 541 p.
[12] V.E. Nazarov. FMM **71**, *3*, 172 (1991).
[13] S.N. Golyandin, K.V. Sapozhnikov, S.B. Kustov. FTT **47**, *4*, 614 (2005).
[14] D. Gelli. J. Appl. Phys. **33**, *4*, 1547 (1962).
[15] S.N. Golyandin, S.B. Kustov, K.V. Sapozhnikov, Yu.A. Emelyanov, A.B. Sinapi, S.P. Nikanorov, W.H. Robinson. FTT **40**, *10*, 1839 (1998).
[16] K.V. Sapozhnikov, S.N. Golyandin, S.B. Kustov. FTT **52**, *1*, 43 (2010).
[17] K.V. Sapozhnikov, S.N. Golyandin, S.B. Kustov. FTT **52**, *12*, 2341 (2010).
[18] V.E. Nazarov, A.B. Kolpakov. J. Acoust. Soc. Am. **107**, *4*, 1915 (2000).
[19] V.E. Nazarov. FMM **88**, *4*, 82 (1999).
[20] D.V. Sivukhin. General physics course. Fizmatlit, M. (2004). V. 3. 656 p. (in Russian).
[21] S. Takizumi. Physics of ferromagnetism. Mir, M. (1987) (in Russian). 420 p. (in Russian).
[22] S.J. Asano. Phys. Soc. Jpn. **29**, *4*, 952 (1970).
[23] A.B. Lebedev. FTT **41**, *7*, 1214 (1999).
[24] V.E. Nazarov, A.V. Radostin. Nonlinear acoustic waves in micro-inhomogeneous solids. Wiley (2015). 251 p.
[25] Lord Rayleigh. Phil. Mag. **23**, 225 (1887).
[26] V.E. Nazarov, S.B. Kiyashko. Non linear dynamics **11**, *4*, 647 (2015).
[27] J.C. Swartz, J. Weertman. J. Appl. Phys. **32**, *10*, 1860 (1961).
[28] L.D. Landau, E.M. Lifshitz. Theory of Elasticity. Nauka, M. (1965).